Appl. Phys. B 51, 285–291 (1990)

Applied Physics B Photophysics and Laser Chemistry

Stimulated Collision Induced Processes in Sodium Vapor in the Presence of Helium*

Z. Konefal and M. Ignaciuk

Institute of Experimental Physics, University of Gdansk, PL-80-952 Gdansk, Poland

Received 23 January 1990/Accepted 11 May 1990

Abstract. Stimulated resonant emission and stimulated Raman effects in sodium vapor in the presence of helium are investigated experimentally. The intensity dependence of these effects on the buffer gas and sodium vapor pressures, and on the intensity and detuning of the exciting radiation are obtained in experiment. Our experimental results agree with the most recent theoretical calculations.

PACS: 32.80. Wr: 32.90. +a

Collision-induced amplified spontaneous emission (ASE) and stimulated electronic Raman scattering (SRS) connected with transitions between excited levels in atomic metal vapor in the presence of collisions had been investigated experimentally [1–3] and analyzed theoretically [4]. The production of ASE on the transition $4^2P_{1/2}$–$4^2S_{1/2}$ (the D_1 line) and SRS connected with the $4^2P_{1/2}$–$4^2P_{3/2}$ transition in a mixture of potassium vapor with helium was first described in [1, 2]. Similar effects in sodium were reported in [3].

The spectrum of the scattered light in a three-level system has been studied by other authors. Carlsten et al. [5] have studied collisional, and recently, Herman et al. [6], radiative effects in three-level systems and the collisional redistribution of near-resonance scattered Raman light. Stimulated emission was observed in potassium–rare-gas mixture by Lemaire et al. [7].

We should mention that the stimulated Raman and stimulated emission effects are applied in several areas of atomic and molecular spectroscopy. The stimulated emission method has been very fruitful in the determination of such fundamental quantities as "weak nuclear charge" in Cs [8], and has allowed the observation of high vibronic levels of molecular ground states [9].

In this paper we report detailed investigations of the ASE and SRS effects in sodium vapor in the presence of helium as a buffer gas. The influence of pump detuning, laser power and sodium and helium pressures on the output ASE and SRS signals are studied. The measurements are in qualitative agreement with the theoretical model described in [4].

1. Three-Level Atom–Light Interaction

We can consider the set of sodium levels $3^2S_{1/2}$–$3^2P_{1/2}$ and $3^2P_{3/2}$ in the presence of collisions as a three-level laser system. This system is shown in Fig. 1. The laser radiation is quasiresonant with the 1–3 transition. The transitions 1–3 and 1–2 are allowed in the dipole approximation. The collision with buffer gas atoms makes the transition between the levels 2 and 3 possible. The ASE

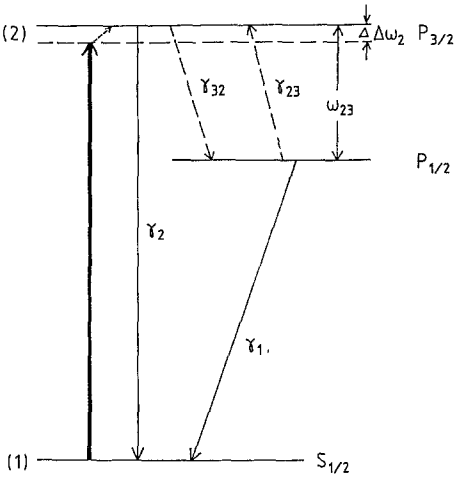

Fig. 1. Simplified energy levels for Na atoms. The straight lines denote radiative decay, broken lines collisional

* This work was carried out under the Polish Central Program of Fundamental Research CPBP 01.06

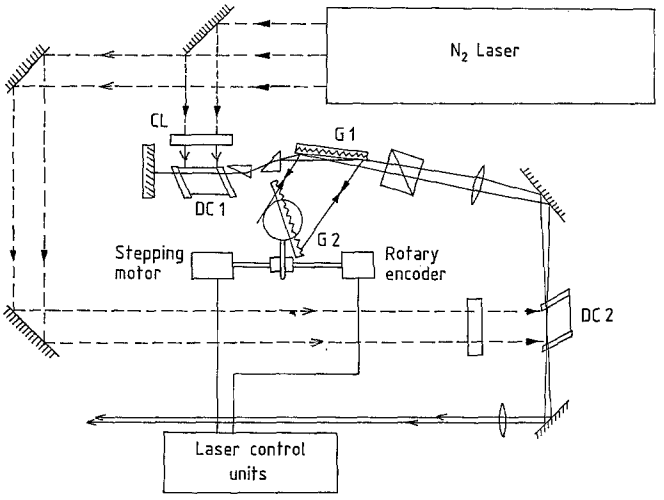

Fig. 2. Schematic of double-grating pulsed dye laser

and SRS effects are caused by effective population of the $3^2P_{1/2}$ level, resulting from collisions of the excited sodium atoms in the $3^2P_{3/2}$ level with the buffer gas atoms during the strong laser pulse. These collisions can lead to inversion of the $3^2P_{1/2}$ level relative to the ground level. This effect can be theoretically explained by the relation:

$$v_{23}=2v_{32}\exp[-(E_3-E_2)/kT],$$

which follows from the detailed balance principle, where v_{32} is the collision transfer rate of the $P_{3/2}$ to $P_{1/2}$ population, while v_{23} corresponds to the opposite process. E_3 and E_2 are the energies of the $P_{3/2}$ and $P_{1/2}$ states respectively, kT is the thermal energy.

2. Experiment

2.1. Dye Laser

We used a dye laser pumped by a home-made a N_2 laser. As illustrated in Fig. 2, the dye laser system is composed of a laser oscillator and a one-stage laser amplifier which are transversely excited. The cavity configuration used a double-prism expander with a 50 mm long 1800 lines/mm grating (Jobin-Yvon) oriented near grazing incidence. A 1200 lines/mm grating in Littrow configuration was used to complete the cavity. The one-stage amplification with excitation power of 500 kW yields an output power up to 10 kW at the oven entrance.

The excitation beam, 2 mm in diameter, was linearly polarized and had a spectral line width of 0.1 cm. Tuning of the laser was accomplished by rotation of a stepping motor, monitored by an absolute rotary encoder of 0.01° resolution. A premonochromator (three prisms mounted at the least-deviation angle) and an aperture prevented unwanted rhodamine fluorescence from entering the cell.

2.2. Cell

Figure 3 shows a vapor cell with a diameter of 2 cm. The cell was made of Pyrex glass of length $l=45$ cm, filled with a mixture of sodium vapor and noble buffer gas. Thermocouples and a temperature controller were used to maintain the temperature to within 1° C. To protect the windows from being coated with Na.

The cell input and output windows were mounted at an angle to avoid back-reflection, which would affect the growth of the stimulated emission. The length of the Na vapor region was 15 cm. A pumping line and gas handling system are used to change the buffer gas pressure.

2.3. Detection System

The experimental apparatus is shown in Fig. 4. The emission of the dye laser was directed into the cell. Mirrors and a beam-splitter were installed in the set-up to investigate the stimulated emission after one or two passes of the laser and ASE and SRS beams through the cell. Radiation leaving the cell was focused onto the entrance of the STE 1 spectrograph.

Instead of a photographic plate, the spectrograph was equipped with a multichannel detector, which will transform a spectrograph into an optical spectrum analyzer (OSA). The detector is the Fairchild CCD 111 monolithic 256-element line image sensor. The CCD sensor is mounted in the film plane of camera body. The commercially available macrophotography equipment allows magnification of the spectrum that appears on the focal plane of the spectrograph. The spectral resolution of the spectrometer-detector system was 0.16 cm^{-1} for each detector diode.

The spectrum from the CCD elements is transferred to the multichannel analyzer (MA) where analog signals from CCD elements are converted to digital. Using the Neptun 184 System Controller the spectrum recorded in

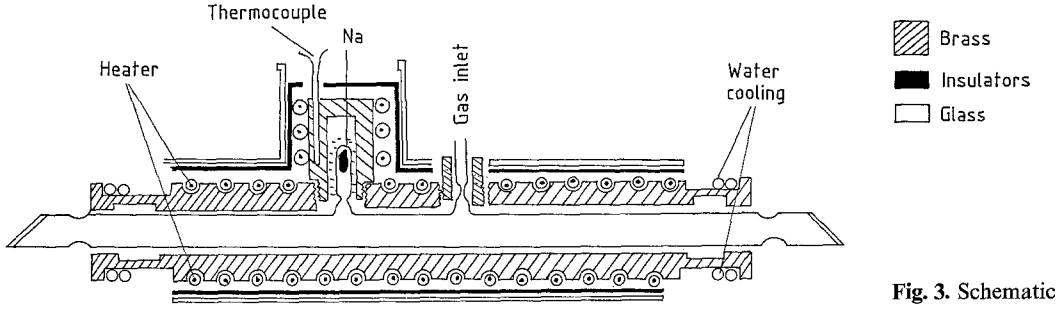

Fig. 3. Schematic diagram of the cell

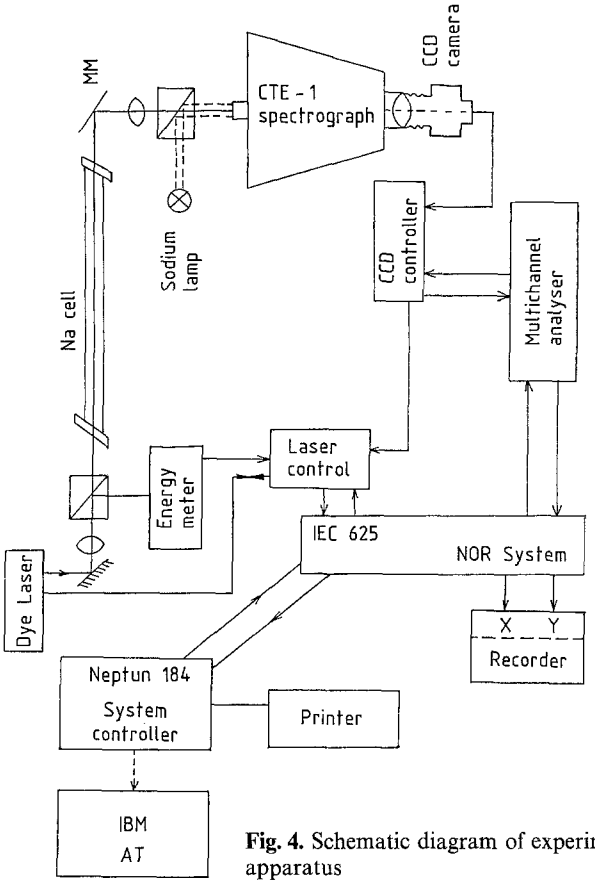

Fig. 4. Schematic diagram of experimental apparatus

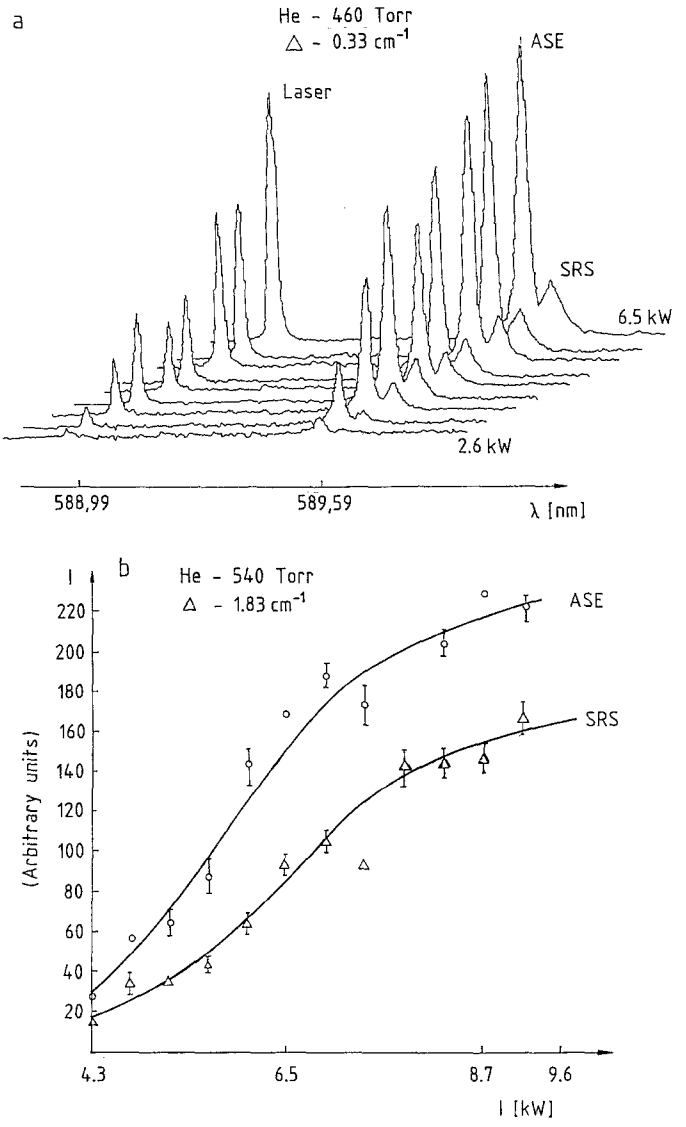

Fig. 5. a Evolution of the spectrum obtained by changing the excitation intensity. **b** Dependence of ASE and SRS energies on the excitation intensity

the MA is sent to a personal computer (IBM AT). The energy meter was also controlled by Neptun 184.

The pulse energy of each laser shot was measured, and spectra were recorded in the computer only if the pulse energy was within a small percentage of a preset value (within 2%). For each spectrum we used 25 laser shots.

The low pressure sodium lamp was used for the precise determination of the position of the ASE, SRS frequency and the excitation frequency.

3. Experimental Results and Discussion

In the experiment, the dependence of the ASE and SRS signals on the intensity and frequency of the exciting radiation, the buffer-gas and sodium-vapor pressure are obtained.

3.1. The Excitation Power Dependence

Figure 5a shows the evolution of the spectrum obtained by changing the power excitation. The excitation intensity was varied from 2.6 kW to 6.5 kW. The temperature of the cell was 311° C, detuning of the exciting radiation frequency (from exact resonance with the D_2 line emitted by the low pressure Na spectral lamp) was 0.33 cm^{-1}. In all cases the excitation laser is tuned to the red side of the D_2 line. The laser beam was focused in the cell to a diameter much smaller than that of the exciting laser beam by a long (40 cm) focal length lens.

Each spectrum is composed of three lines. The first line from the left is the excitation laser line, the central line is the ASE line and the last line originates from SRS. From this spectrum we can see that the ASE and SRS lines increase with increasing laser intensity. The spectrum was taken with a double pass cell configuration (DP).

Figure 5b shows the dependence of the ASE and SRS emission energies on the exciting-radiation intensity. The cell temperature is 341° C, detuning 1.83 cm^{-1} and helium pressure 540 Torr. This dependence was obtained using one pass cell configuration, whereas all other results were measured with the DP configuration.

As can be seen from Fig. 5b, both the ASE and SRS emissions grow linearly at low intensities, grow exponentially when the scattering becomes stimulated at higher intensity until saturation occurs. In this case the ASE and SRS outputs are limited by the available number of initial state atoms (atom depletion) [10]. Similar results were

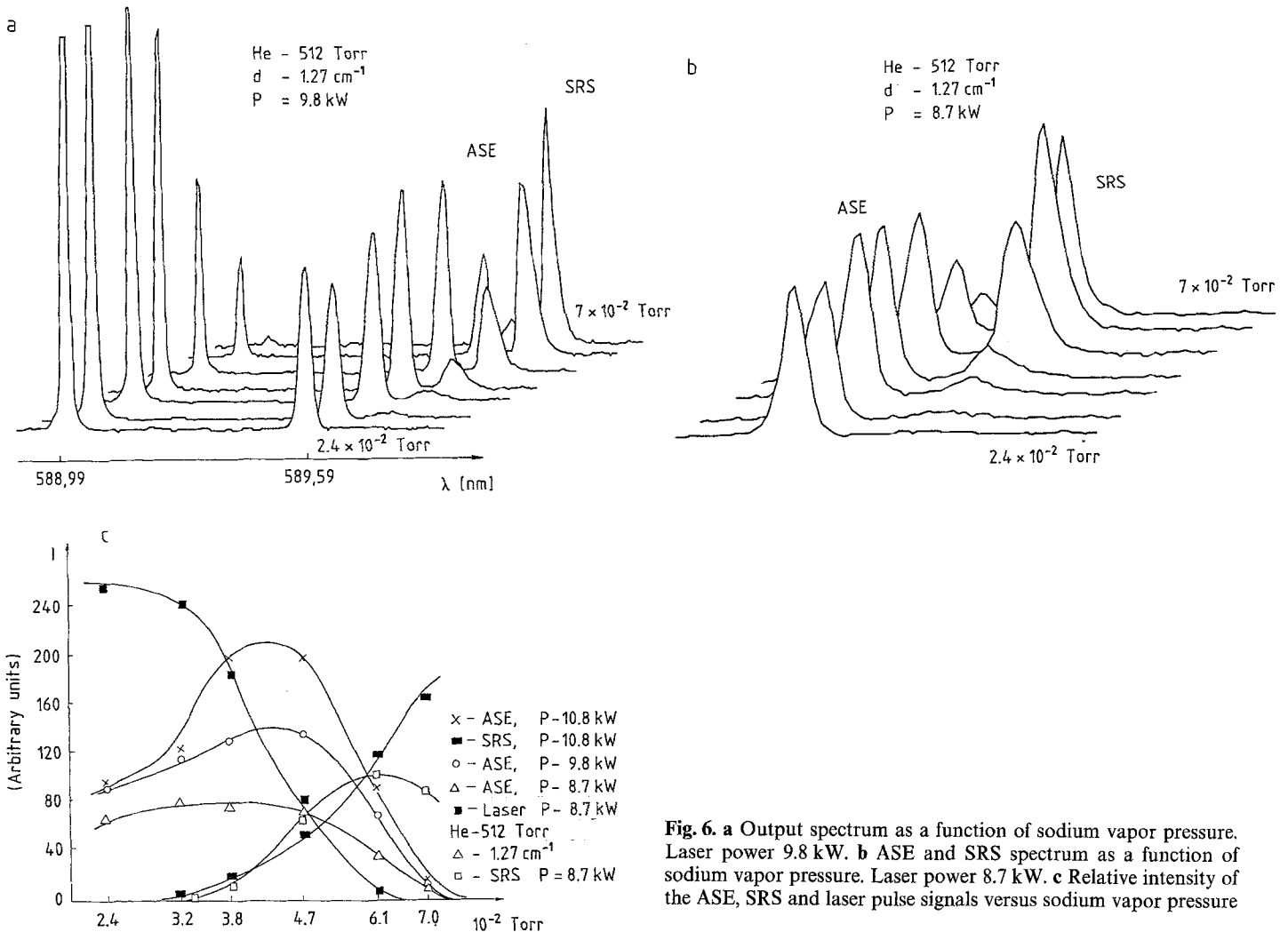

Fig. 6. a Output spectrum as a function of sodium vapor pressure. Laser power 9.8 kW. **b** ASE and SRS spectrum as a function of sodium vapor pressure. Laser power 8.7 kW. **c** Relative intensity of the ASE, SRS and laser pulse signals versus sodium vapor pressure

obtained by Raymer and Carlsten [11] in thallium. From Fig. 5b we can see that in the double-pass configuration the SRS intensity is comparable with ASE intensity.

3.2. Sodium Vapor Pressure Dependence

Figure 6a shows the output spectrum as a function of sodium vapor pressure. The pressure was varied between 2.4×10^{-2} Torr (309° C) and 7×10^{-2} Torr (340° C). The buffer-gas pressure was 512 Torr, detuning 1.27 cm^{-1} and laser intensity 9.8 kW.

Several important features can be observed.

1) The exciting laser pulse for the low temperature had enough energy after passing the cell twice to saturate the CCD elements. When we increase the sodium-vapor pressure, the energy of the laser pulse is absorbed strongly in the cell. Therefore the pump laser line intensity decreased with increasing cell temperature. It can be seen from Fig. 6a that the 9.8 kW laser pulse is almost completely absorbed at 340° C (7×10^{-2} Torr).

2) As we had rather high helium pressure in the cell and the system was pumped by a high power laser pulse, the ASE signal appeared at relatively low sodium-vapor pressure. At 309° C the intensity of the ASE signal is rather strong. The ASE signal increases with the increase of the cell temperature. When the sodium vapor pressure is raised to about 4×10^{-2} Torr the ASE energy increases to a maximum. For the higher sodium-vapor pressure, when the pump laser pulse is absorbed almost completely in the cell, the intensity of the ASE signal decreases with the further increase of the temperature. The decrease of the ASE signal is apparently due to absorption of the ASE photons in the end of the cell where the pump signal is too small to build up a population inversion of the $P_{1/2}$ state with respect to the $S_{1/2}$ ground state. The ASE signal is in resonance with the $P_{1/2}$–$S_{1/2}$ transition.

3) In the SRS case, this signal is not in resonance with any real transition. That is why the maximum for that signal is shifted to higher sodium-pressure region. This is exactly what has been observed for potassium [1]. Under this experimental condition, when the pressure of the buffer-gas is higher, the SRS signal appears at higher sodium-vapor pressure than ASE.

At constant dye laser power (9.8 kW) the Stokes output was seen to rise rapidly at the higher sodium pressures. From Fig. 7a we can see that in this region the depletion of the pump power by ASE is negligible. From this spectrum we can see also that the bandwidth of the Stokes radiation decreases with increasing sodium pres-

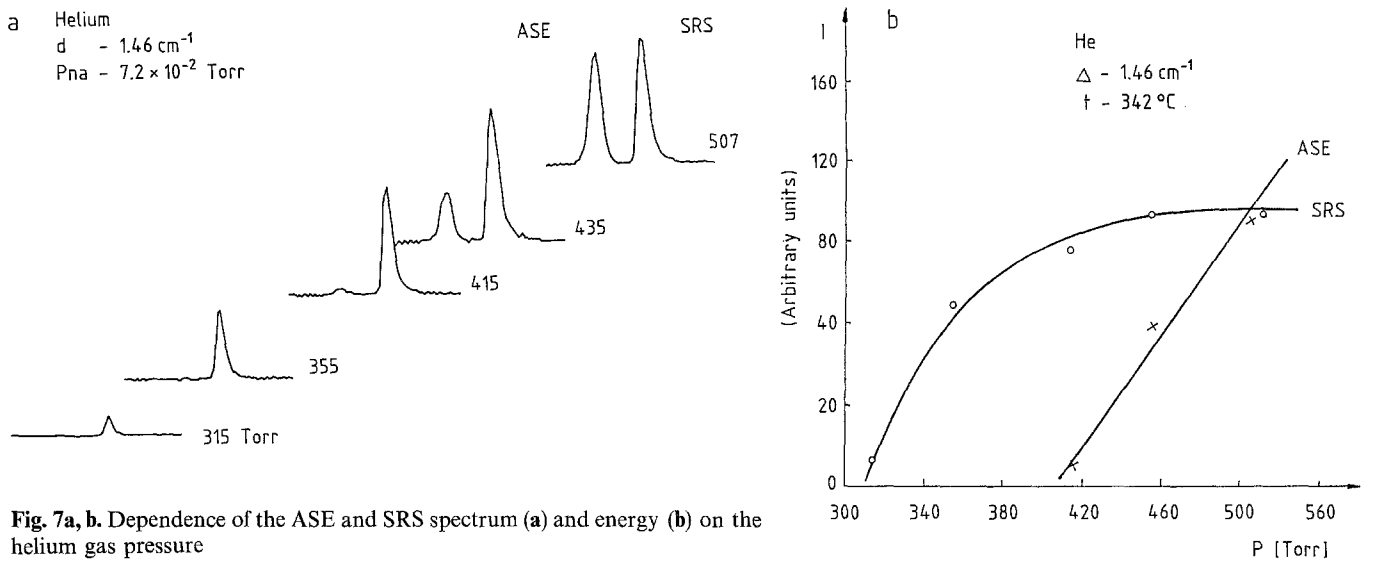

Fig. 7a, b. Dependence of the ASE and SRS spectrum (**a**) and energy (**b**) on the helium gas pressure

sure. The width (FWHM) of the SRS signal changes from 1.28 cm^{-1} to 0.72 cm^{-1} as the sodium vapor pressure varies from 3.8×10^{-2} to 7×10^{-2} Torr. This effect can be explained by taking into account the fact that the decrease in ASE signal with increasing sodium pressure should increase the effective generation time of the Raman signal, thus resulting in a narrowing of the linewidth. High time resolution experiments will provide the answer to the above plausible interpretation. These were not performed in the present work.

Figure 6b shows the ASE and SRS spectrum as a function of sodium vapor pressure. The laser power is 8.7 kW. For this laser power, when the sodium vapor pressure is raised to 6×10^{-2} Torr the SRS energy increases to a maximum. For higher sodium pressures we observed a decrease of SRS energy. This decrease of the SRS energy with increasing sodium-vapor pressure is apparently due to the increase of the optical thickness of the absorption layer.

Figure 6c shows the relative intensity of the ASE, SRS and laser lines versus sodium-vapor pressure for different laser excitation intensities. From this figure, one can see much more clearly the dependence of the ASE and SRS signals on the laser intensity and cell temperature which was discussed above. The SRS signal strongly depends on sodium vapor density. As can be seen from Fig. 6a, the SRS signal appears only for high cell temperature. For the 10.8 kW laser pulse and 512 Torr helium pressure, the SRS signal can be seen from 3.2×10^{-2} Torr sodium vapor pressure (322° C). From Fig. 6b we can see that the maximum value of ASE signal strongly depends on pump power. When we change this by 20% (from 8.7 kW to 10.8 kW), the intensity of that signal doubles for the optimum value of sodium-vapor density.

3.3. *The Buffer-Gas Dependence*

The dependence of the ASE and SRS spectrum on the helium-gas pressure is shown in Fig. 7a. From this spectrum we see that for small buffer-gas pressure, high sodium pressure and large detuning (1.46 cm^{-1}), the SRS signal first appear at 315 Torr of helium but the ASE signal appears at 415 Torr helium pressure. The threshold pressure for ASE signal strongly depends on laser detuning. For small detuning we find a threshold value for ASE of 180 Torr.

The SRS signal increases almost linearly with pressure up to 360 Torr, but above this value the signal becomes nonlinear and for pressures higher than 450 Torr it saturates. To saturate the ASE signal we should use much higher pressure of helium.

The experimental dependence of the ASE and SRS energies on the helium gas pressure is shown in Fig. 7b. From this figure we can see that the Raman component appears in the low pressure region even when the ASE component is absent, but the intensity of the ASE increases almost linearly with helium pressure and for higher pressures, the ASE component is much intense than the Raman component. These two results (dependence of ASE signal on laser detuning and on buffer-gas pressure) are confirmed by the theoretical calculation [4].

3.4. *Laser Detuning Dependence*

Finally, we want to discuss the dependence of ASE and stimulated Raman intensities on detuning for a given pressure and laser intensity. Figure 8a shows the dependence of the ASE and SRS spectrum on the laser detuning. Figure 8b shows the intensities of the ASE and SRS components of the Na spectrum as a function of the detuning. It can be seen that with increasing detuning, the ASE component first increases and after passing through a maximum value it decreases and disappears when the laser is detuned by more that 2 cm^{-1} from resonance. The Raman component also decreases monotonically with increasing detuning but is present even when the ASE component disappears. These results were obtained with a 342° C cell temperature. For this temperature we cannot obtain any spectrum for less the 1 cm^{-1} laser detuning.

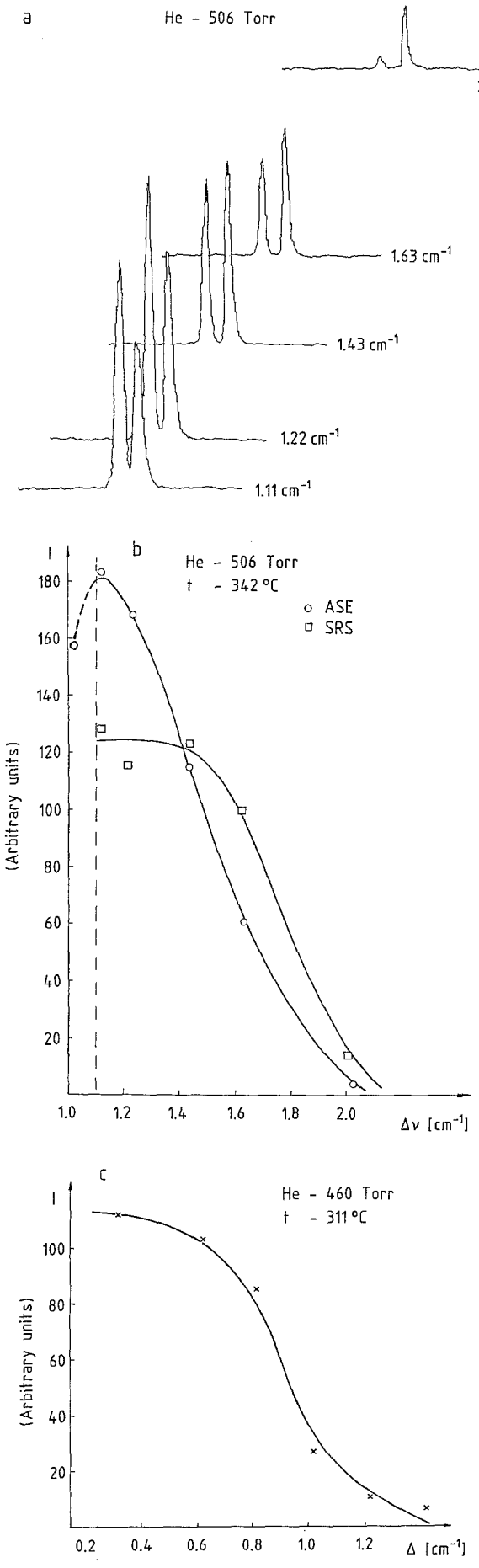

This is due to the self-focusing effect. For the low sodium-vapor pressure (Fig. 8c), the ASE signal appears when detuning from the resonance is about 0.2 cm^{-1}. Strong defocusing was observed for tuning closer to resonance. It is known that the self-focusing effect strongly depends on sodium density and increases with increasing pump power.

Unfortunately, we cannot obtain any spectrum connected with blue shifts of the excitation frequency. This is also due to the self-focusing effect which appears on this side of the D_2 line. Javan and Kelly [12] predicted that a simple, homogeneously or inhomogeneously broadened two-level atomic absorber would cause wavelength-dependent focusing. What we observe for sodium is qualitatively consistent with this behavior. It is known from [13] that self-focusing in sodium vapor can be enhanced when buffer gas is introduced. This is the only explanation of the unusual effect observed in [3] connected with the asymmetry of the ASE energies with respect to excitation frequency. This result obtained by Atutov et al. [3] is also in disagreement with the theoretical results of Czub et al. [4]. A similar asymmetry of the line was observed by Kolwas and Kolwas [14].

4. Conclusion

A detailed study of collision-aided stimulated processes in sodium vapor in the presence of helium has been presented. The results on pump detuning and intensity and on the helium and sodium-vapor pressures are in qualitative agreement with the theoretical model based on the dressed atom density matrix approach.

We have seen the growth of both components from spontaneous to stimulated scattering as the laser intensity increases. Our results show that when the buffer gas pressure is high enough (above 500 Torr) and laser detuning is small, the ASE component appears first. For the low buffer-gas pressure (above 300 Torr) and large laser detuning, the SRS signal appears first. The intensity of the SRS signal reaches its maximum for higher sodium vapor pressure than the ASE signal intensity. For low sodium-vapor pressure only the ASE signal is generated. The strong ASE signal which first appears markedly reduces the effective population of the Raman level, leading to a broadening of the SRS signal.

Preliminary results also show that the ASE signal can be used for very precise determination of the pressure shift of the D_1 line. The measurements show strong threshold pressure dependence of ASE and SRS signals on the type of buffer gas. We believe that this fact can be used to determine the sodium–noble-gas interaction.

The advantages of techniques using the ASE and SRS signals come from two facts:

Fig. 8. a Dependence of ASE and SRS spectrum on laser detuning; **b** intensities of the ASE and SRS components of Na spectrum as a function of the laser detuning. Cell temperature 342° C; **c** intensity dependence of the ASE signal as a function of laser detuning. Cell temperature 311° C

1) The stimulated emission of the atoms forms an easily detected beam of radiation, which is of short duration and well collimated;

2) The excited atoms are very rapidly deexcited due to the large stimulated emission probability and therefore single-collision conditions can be achieved even at high gas pressure.

References

1. A.A. Dabagyan, M.E. Movsessyan, T.H. Ovakimyan, S.V. Shmavonyan: Zh. Eksp. Teor. Fiz. **85**, 1203 (1983)
2. A.A. Dabagyan, M.E. Movsessyan, T.H. Ovakimyan, S.V. Shmavonyan: Izv. Akad. Nauk SSSR Fiz. **47**, 1609 (1983)
3. S.N. Atutov, A.I. Plekhanov, A.M. Shalagin: Opt. Spectrosk. **56**, 215 (1984)
4. J. Czub, J. Fiutak, W. Miklaszewski: Z. Phys. D **3**, 23 (1986)
5. J.L. Carlsten, A. Szoke, M.G. Raymer: Phys. Rev. A **15**, 1079 (1977)
6. B.J. Herman, J.H. Eberly, M.G. Raymer: Phys. Rev. A **39**, 3447 (1989)
7. J.L. Lemaire, W.-ÜL. Tchang-Brillet, F. Rostas: In *Spectral Line Shapes*, ed. by R.J. Exton (A Deepak Publishing 1987)
8. M.A. Bouchiat, J. Guena, Ph. Jacquier, M. Lintz, L. Pottier: Proc. ELICAP "Atomic Physic 11" ed. by S. Haroche, J.C. Gay, G. Grynberg (Word Scientific, Singapore 1989)
9. M. Broyer, G. Delacretaz, G.Q. Ni, R.L. Whetten, J.P. Wolf, L. Woste: Phys. Rev. Lett. **62**, 2100 (1989)
10. D. Cotter, D.C. Hanna: IEEE J. QE-**14**, 184 (1978)
11. M.G. Raymer, J.L. Carlsten: Phys. Rev. Lett. **39**, 1326 (1977)
12. A. Javan, P.L. Kelly: IEEE J. QE-**2**, 470 (1966)
13. G. Grynberg, P. Verkerk: Opt. Commun. **61**, 296 (1987)
14. K. Kolwas, M. Kolwas: Z. Phys. A **321**, 207 (1985)